Potential Description of α+^{208}Pb Elastic Scattering

M Nure Alam Abdullah, M Zahid Hasan, Sinthia Binte Kholil and Dipika Rani Sarker

Department of Physics, Jagannath University, Dhaka-1100 Bangladesh

LXX International Conference "NUCLEUS-2020. Nuclear physics and elementary particle physics. Nuclear physics technologies"

Introduction

- Nuclear structure → nucleus-nucleus interaction potential
- Nuclear scattering due to nuclear forces (to analyse the experimental angular distribution of the emitted particles)

  ↓

  Nuclear potential

- The optical model (OM) potential is pretty well known to explain the phenomena.
- Alpha-particle elastic scattering → ALAS (Anomaly in Large Angle Scattering)
- ALAS is prominent but not unique to A ≈ 4n (n = 1, 2, 3, …) nuclei and for A ≤ 50.
- Beyond this region, the ALAS effect rapidly dies down giving rise to the "rainbow scattering".

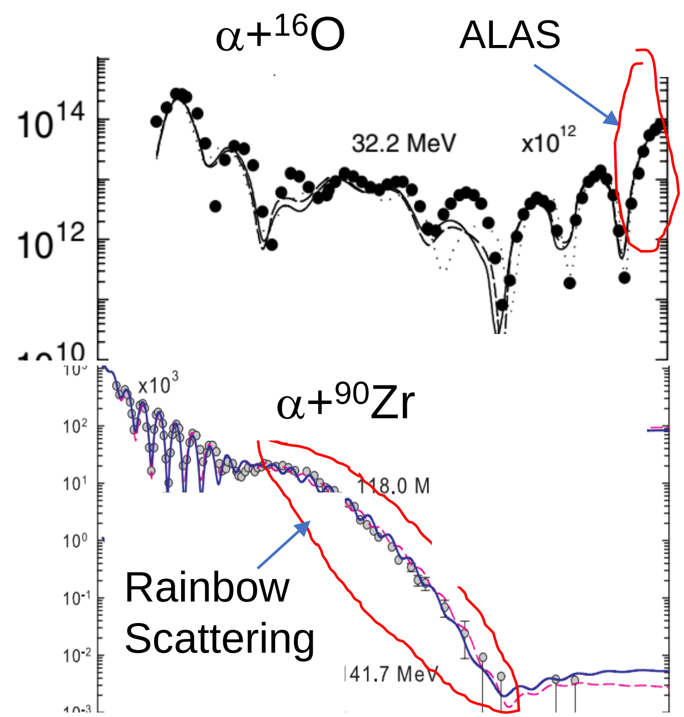

K.W. Kemper, A.W. Obst and and R.L. White, Phys. Rev. C 6 (1972) 2090.
L. Jarczyk et al., Acta Phys. Pol. B 7 (1976) 53.

Introduction

Optical model (OM) potential

Phenomenological OM potential
(obtained empirically from the direct analysis of the elastic scattering data)

↓

(i) Woods-Saxon (WS)
(ii) squared Woods-Saxon (SWS)

Problem → suffer from discrete and continuous ambiguities

OM potentials is derived microscopically or semi-microscopically

↓

(i) Folded (both double-folded and single-folded)
(ii) non-monotonic (NM) - derived from the EDF theory of Brueckner, Coon and Dabrowski (BCD).

K.W. Kemper, A.W. Obst and R.L. White, Phys. Rev. C 6 (1972) 2090.
F. Michel et al, Phys. Rev. C 28 (1983) 1904.

M. E. Brandan and G. R. Satchler Phys. Rep. 285 (1997) 143.
M. N. A. Abdullah et al, Eur Phys J. A 18 (2003) 65
M. N. A. Abdullah et al, Nucl. Phys. A 760 (2005) 40.
K. A. Brueckner, S. A. Coon and J. Dabrowski, Phys. Rev. 168 (1968) 1184.

Introduction

- Traditional double folded (DF) of effective *N-N* interaction and single folded (SF) of either α-*N* or α–α potentials need renormalizations at different incident energies.

- In 2003, we proposed a single-folding model the resulting potential from which does not need any renormalization.

- *M. N. A. Abdullah et al., Eur. Phys. J. A 18 (2003) 65.*
- *M. N. A. Abdullah et al., Phys. Lett. B 571 (2003) 45.*

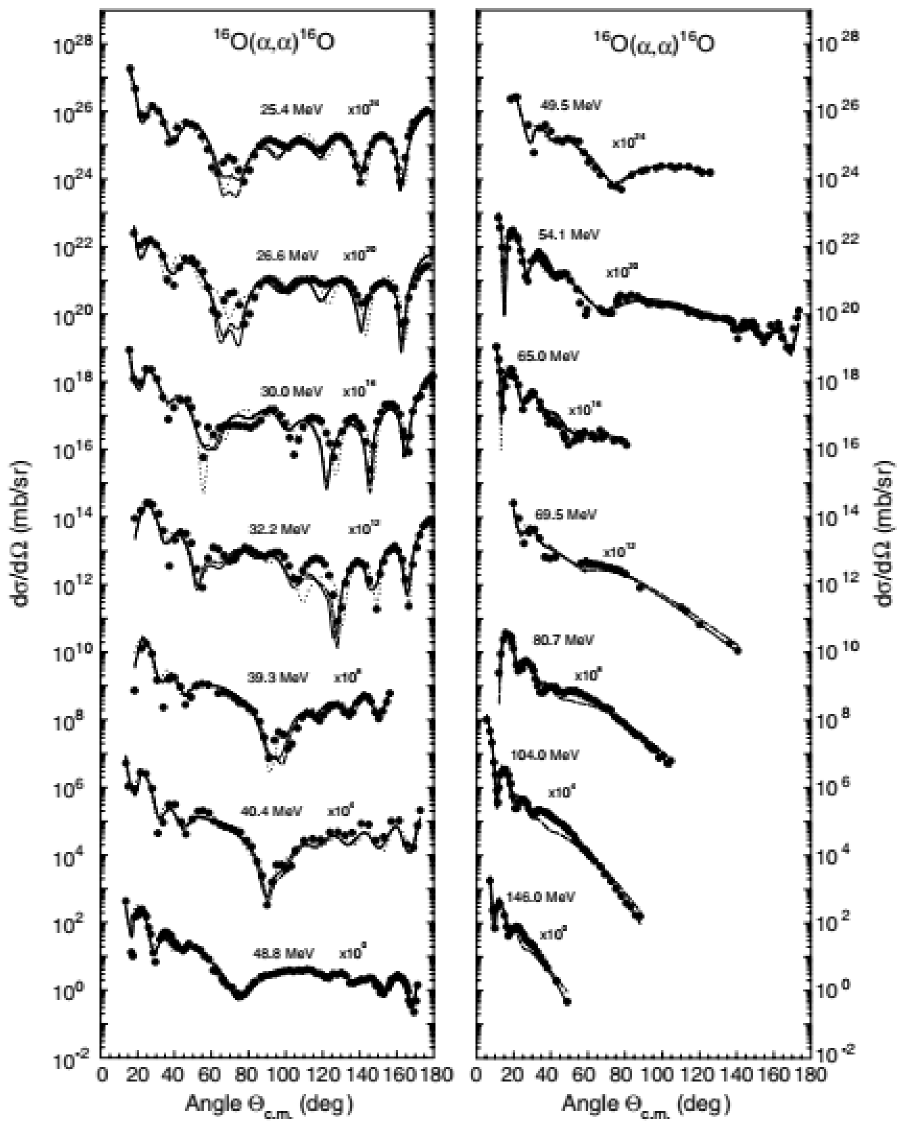

M. N. A. Abdullah et al., Eur. Phys. J. A 18 (2003) 65

Our Folding Model

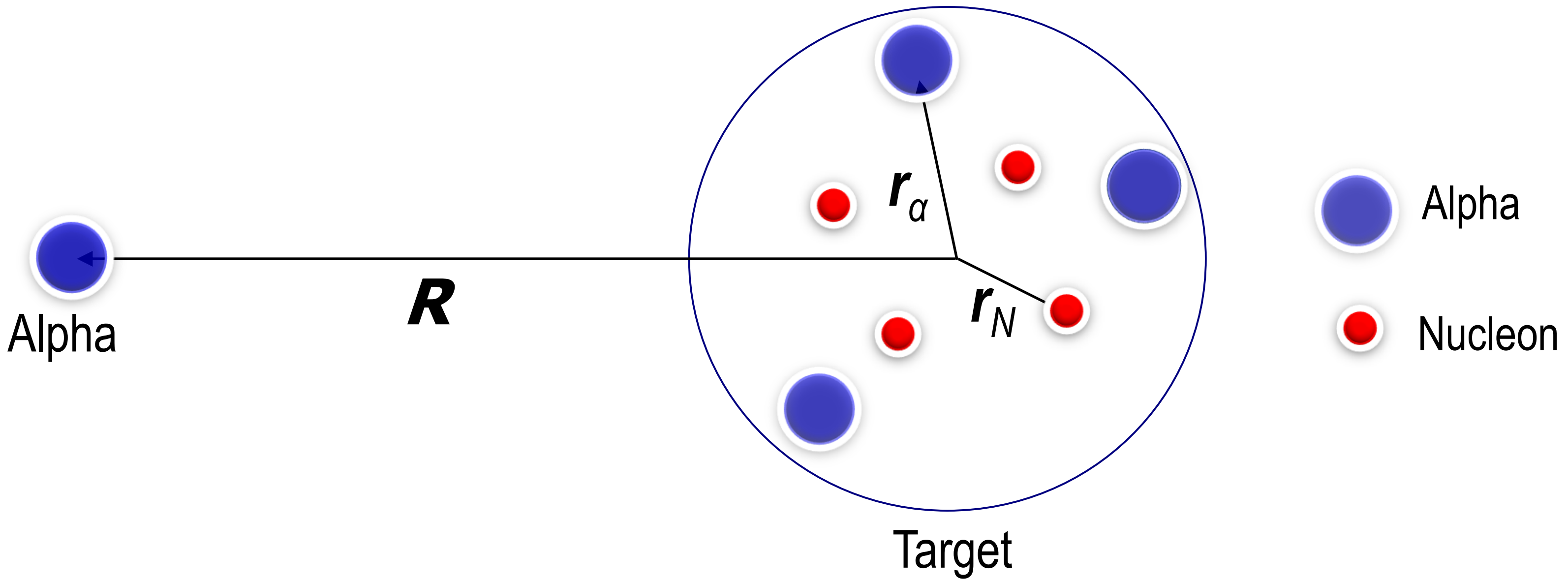

Assumptions:

i. the nucleons in the target are considered primarily in the α–cluster configuration, and rest in an unclustered nucleonic configuration

ii. the wave function of a nucleus can be considered as the product of wave functions of α-like configurations and those of unclustered nucleonic configurations

iii. This leads to a sum of two folding potentials, one convoluted over α-density distribution and another over nucleonic density distribution.

MSF Potential

The modified single folded (MSF) real nuclear potential:

$$U(R) = \int \rho_\alpha(\vec{r}_\alpha) V_{\alpha\alpha}\left(\left|\vec{R} - \vec{r}_\alpha\right|\right) d^3\vec{r}_\alpha + \int \rho_N(\vec{r}_N) V_{\alpha N}\left(\left|\vec{R} - \vec{r}_N\right|\right) d^3\vec{r}_N. \quad (1)$$

α–α potential: $V_{\alpha\alpha}(r) = V_R\, exp(-{\mu_R}^2 r^2) - V_A\, exp(-{\mu_A}^2 r^2)$. (2)

α–N potential: $V_{\alpha N}(r) = -V_0\, exp(-k^2 r^2)$. (3)

The parameter values are:

V_A = 122.62 MeV, μ_A = 0.469 fm^{-1}

[*B. Buck, H. Friedrich, C. Wheatley, Nucl. Phys. A 275 (1977) 241.*]

V_0 = 47.3 MeV and K = 0.435 fm^{-1}

[*S. Sack, L. C. Biedenharn, G. Breit, Phys. Rev. 93 (1954) 321.*]

Density distribution used:

$$\rho_i(r) = \rho_{0i}\left[1 + exp\left(\frac{r - c_i}{a_i}\right)\right]^{-1}, \text{ with } i = \alpha, N \quad (4)$$

MSF Potential

The Imaginary potential: $W(R) = -W_0\, exp\left(-\frac{R^2}{{R_W}^2}\right)$. (5)

Coulomb potential: $$V_C(R) = \begin{cases} \frac{Z_1 Z_2 e^2}{2R_C}\left(3 - \frac{R^2}{{R_C}^2}\right), & R \leq R_C \\ \frac{Z_1 Z_2 e^2}{2r}, & R > R_C. \end{cases}$$ (6)

with $R_C = 1.35 \times A^{1/3}$.

Normalization integral: $\int \rho_\alpha(\vec{r}_\alpha) d^3\vec{r}_\alpha + \int \rho_N(\vec{r}_N) d^3\vec{r}_N = 4A_\alpha + A_N = A_T$. (7)

Non-monotonic (NM) potential

The analytic form of the NM potential:

Real part:

$$V_{NM}(r) = -V_0\left[1 + exp\left(\frac{r - R_0}{a_0}\right)\right]^{-1}$$
$$+V_1 exp\left[-\left(\frac{r-D_1}{R_1}\right)^2\right] + V_C(r) \qquad (9)$$

The potential becomes non-monotonic with the inclusion of the second term.

Imaginary part:

$$W_{NM}(r) = -W_0 exp\left[-\left(\frac{r}{R_W}\right)^2\right]$$
$$-W_S exp\left[-\left(\frac{r-D_S}{R_S}\right)^2\right]. \qquad (10)$$

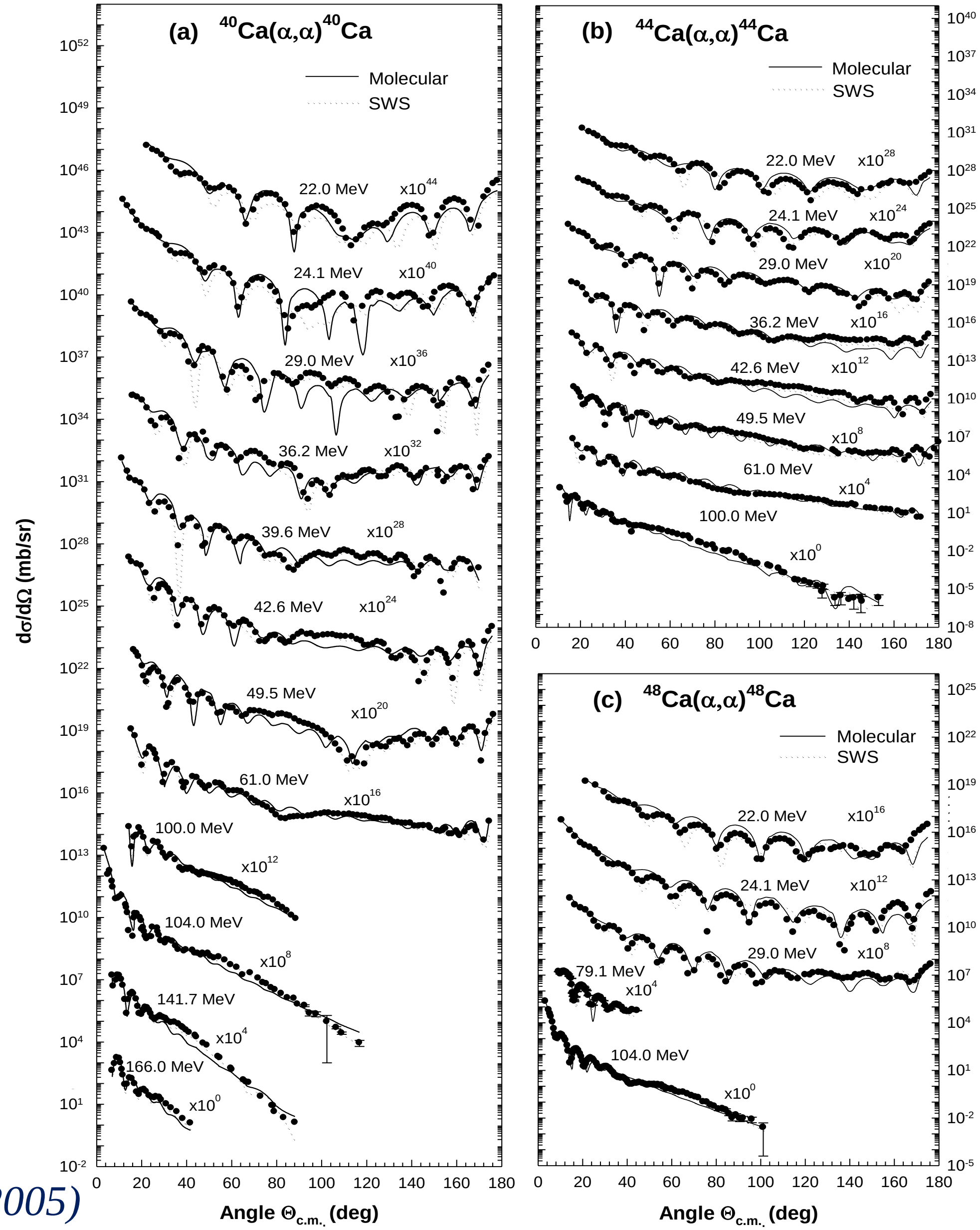

[M. N. A. Abdullah et al, Nucl. Phys. A 760 (2005) 40.]

Non-monotonic (NM) potential

- Hossain *et al*. was able to explain the refractive structure of α+^{90}Zr elastic scattering using the NM potential derived from the EDF theory.

- The potential in the central region of the target nucleus seems to be significant in describing the α elastic scattering data on ^{90}Zr.

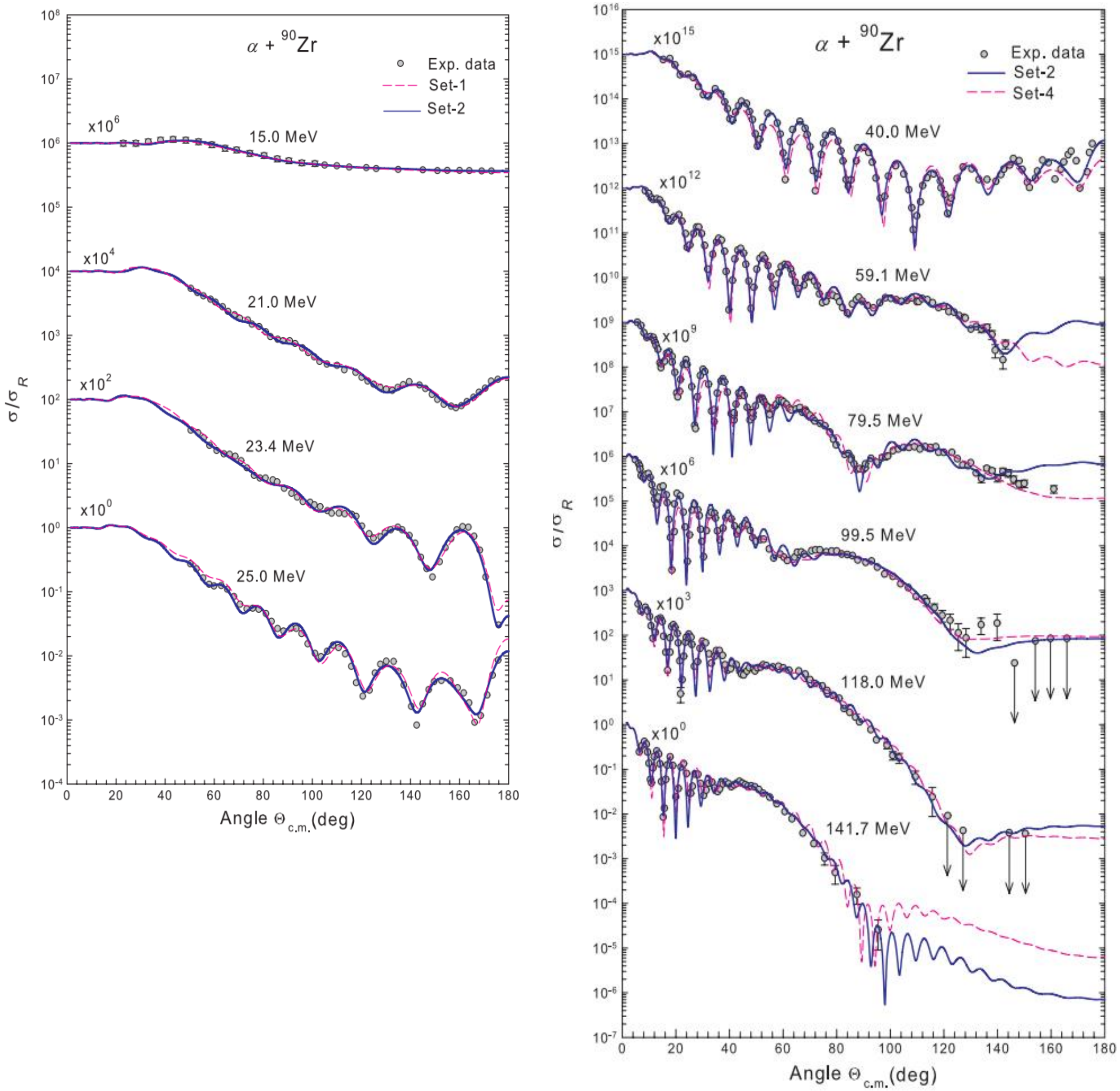

S. Hossain et al, J. Phys. G: Nucl. Part. Phys. 40 (2013) 105109.

Non-monotonic (NM) potential

Basak *et al.* successfully extended the approach of using the NM potential, derived from a realistic two-nucleon (NN) potential using the EDF method, to reproduce simultaneously

- the elastic scattering cross-sections and
- the vector analyzing power data for $^{6,7}Li$ projectiles on ^{12}C, ^{26}Mg, ^{58}Ni and ^{120}Sn
- without adjusting the shape or depth parameters of the EDF-derived potentials.

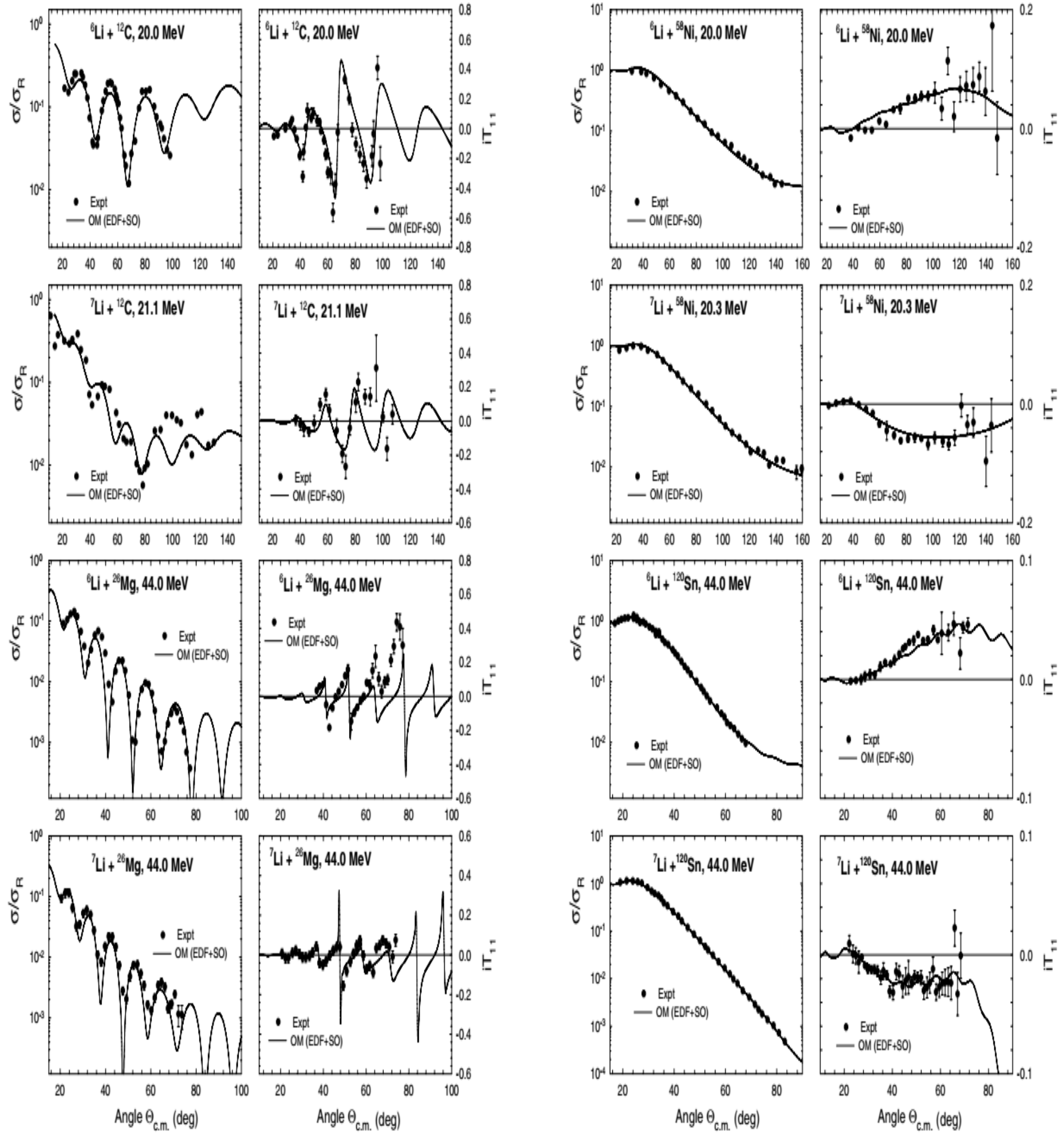

A. K. Basak et al, Europhys. Lett. 94 (2011) 62002.

Non-monotonic (NM) potential

Strikingly, their analysis correctly described the observed opposite signs in the elastic scattering VAP data for ^{6}Li and ^{7}Li of the same energy incident on ^{58}Ni and ^{120}Sn nuclei.

These successes are attributed to the following features:

(i) the NM nature of the central real potential arising from the use of the Pauli effect in the EDF theory

(ii) optimum use of empirical absorption

(iii) an appropriate choice of the effective SO potential of either sign, being a manifestation of the projectile excitation process.

Analysis

Code used:

SCAT2 *[O. Bersillon, The code SCAT2, NEA 0829, private communication.*

SFRESCO which incorporates the coupled-channels code FRESCO 2.5
[*I. J. Thompson. Comp. Phys. Rep. 7 (1988) 167.]*

MINUIT [*F. James and M. Roos, Comp. Phys. Commun. 10 (1975) 343.]*

A set of parameters is obtained by minimizing χ^2 defined as:

$$\chi^2 = \frac{1}{N}\sum_i \left[\frac{\sigma_{exp}(\Theta_i)-\sigma_{th}(\Theta_i)}{\Delta\sigma_{exp}(\Theta_i)}\right]^2. \qquad (8)$$

Results of MSF

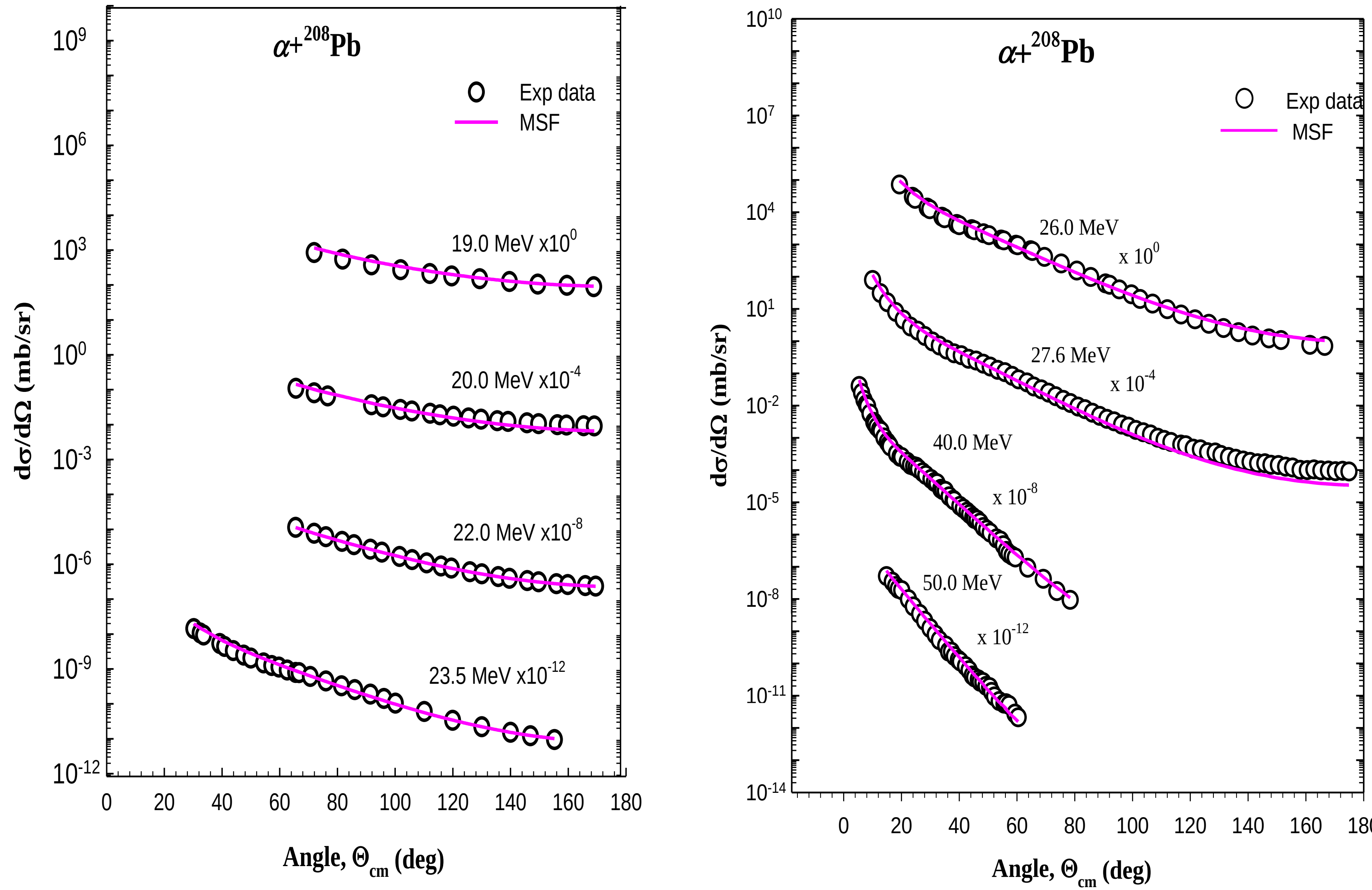

Fig. 2. The predicted cross sections for the $\alpha+^{209}Pb$ elastic scattering using the MSF potentials at E_α = 19.0-50.0 MeV. The open circles are the experimental data.

Results of MSF

Table 1. Energy independent parameters and the deduced results for α+^{208}Pb elastic scattering. $\rho_{0\alpha}$ and ρ_{0N} are in fm^{-3}; c_α, c_N, $a_\alpha = a_N$ and R_{rms} in fm.

Target	$\rho_{0\alpha}$	ρ_{0N}	c_α	c_N	$a_\alpha = a_N$	$4A_\alpha$	A_N	A_T	R_{rms}
^{208}Pb	0.0347	0.192	6.62	3.0	0.546	180.0	28.0	208	5.514

Table 2. Energy dependent parameters along-with the volume integrals and χ^2. E_a, and the depth parameters V_R and W_0 are in MeV; μ_R in fm^{-1}; R_W in fm; and $J_R/(4A)$ and $J_I/(4A)$ in MeV.fm^3.

E_α	V_R	μ_R	W_0	R_W	$J_R/(4A)$	$J_I/(4A)$	χ^2
19.0	15.0	0.60	18.0	7.20	-397.4	-41.52	1.81
20.0	20.0		19.0		-391.1	-43.83	1.74
22.0	25.0		24.0		-384.8	-55.36	0.31
23.5	30.0		29.0		-378.4	-66.90	2.59
26.0	40.0		40.0		-366.0	-92.27	3.57
27.6	50.0		40.0		-353.5	-92.27	7.57
40.0	55.0		42.0		-347.2	-96.88	3.86
50.0	65.0		45.0		-328.5	-103.8	3.78

Results of NM

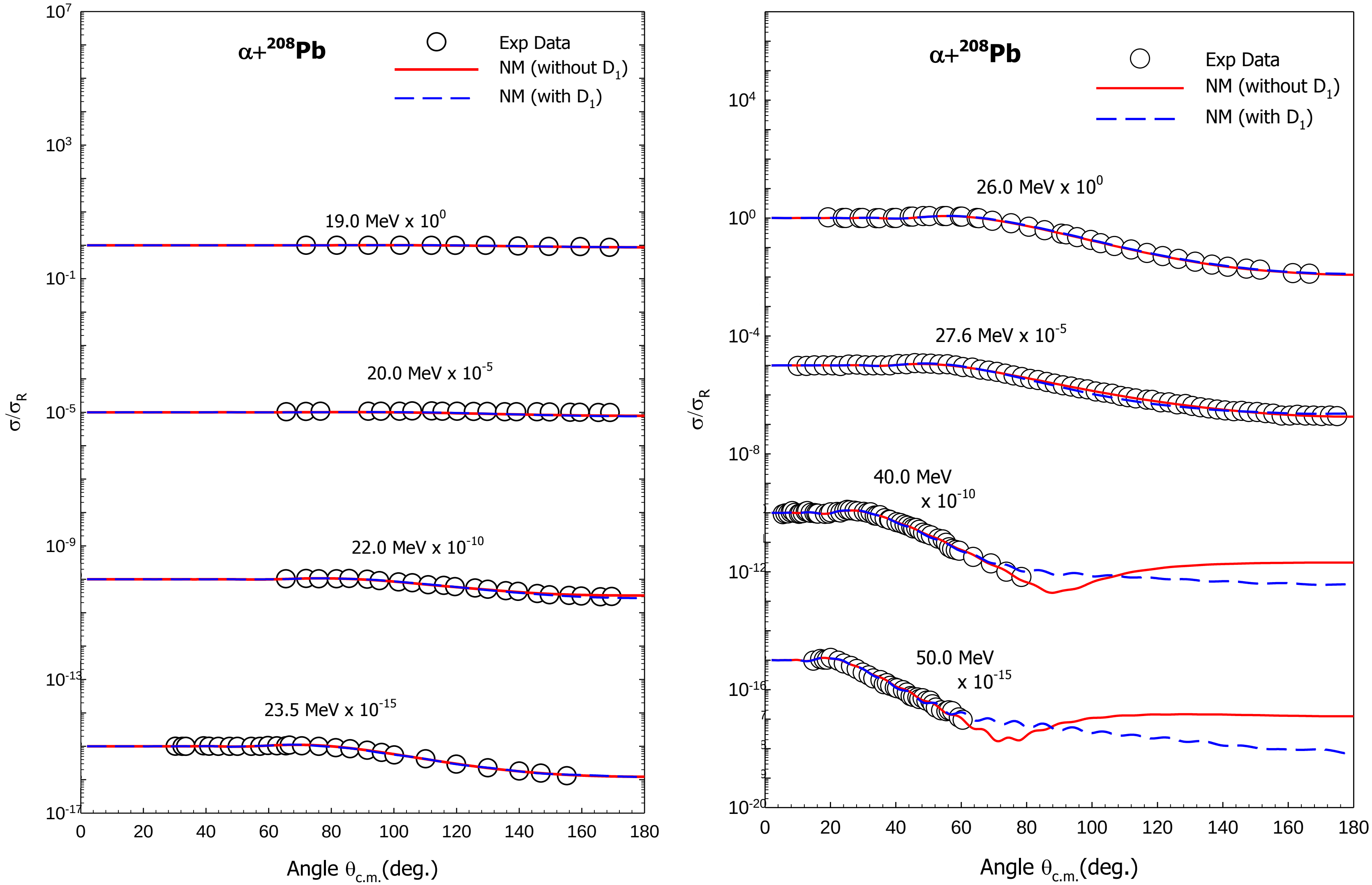

Fig. 3. The predicted cross sections for the α+^{209}Pb elastic scattering using the NM potentials with unshifted repulsive core (green broken lines) and shifted repulsive core (red solid lines) at E_α = 19.0-50.0 MeV are compared to the experimental data (open circles).

Results of NM

Table 3. The real part of the NM potentials for the fits to the α+[208]Pb elastic scattering at E_α = 19.0 – 50.0 MeV. V_0 and V_1 in MeV, and R_0, a_0, D_1, R_1 and R_C in fm.

Set	V_0	R_0	a_0	V_1	D_1	R_1	R_C	$J_R/(4A)$
Set-1 (D_1 = 0)	11.49	7.674	0.2876	141.7	0.00	2.610	10.5	-100.0
Set-2 ($D_1 \neq 0$)	14.50	7.3648	0.3650	40.465	2.00	2.60	10.5	-100.0

Table 4. The imaginary parameters of the NM potentials for fits to the α+[208]Pb elastic scattering data. W_0 and Ws are in MeV; R_S, R_W, D_S in fm; $J_I/(4A)$ in MeV.fm^3.

E_α	Set-1 (D_1 = 0)							Set-2 ($D_1 \neq 0$)						
	W_0	R_W	W_S	D_S	R_S	$J_I/(4A)$	χ^2	W_0	R_W	W_S	D_S	R_S	$J_I/(4A)$	χ^2
19.0	15.0	1.0007	5.20	6.450	1.5874	-99.45	0.014	10.0	1.0007	2.20	6.445	1.587	-42.35	0.0060
20.0							1.102							0.919
22.0							0.089							0.085
23.5							0.151							0.055
26.0	38.9	1.0409	2.75	6.3954	1.2946	-44.35	0.057	40.0					-44.45	0.115
27.6	129.5	1.0007	8.37	6.450	1.5874	-167.31	0.0617	25.0		3.20			-62.32	0.787
40.0			5.20			-107.06	0.376	32.0		3.20			-62.81	1.01
50.0			8.80			-175.16	1.896	30.0		5.20			-100.50	2.69

Discussion and Conclusions

- Both the MSF and NM potentials satisfactorily describe the $\alpha+^{209}Bi$ elastic scattering data.
- However, the MSF potential slightly underestimates the cross sections at 27.6 MeV. This may be due to the lack of proper density parameters. To the best of our knowledge, there is no density distributions available in the literature for ^{208}Pb and as so we have used density distribution of ^{207}Pb.
- The derived MSF potential does not need any renormalization for a satisfactory description of the data over the entire energy range.
- The addition of the repulsive component conforms to the Pauli exclusion principle.
- The radius c_N = 3.0 fm of the unclustered nucleonic distribution is much less that c_α = 6.62 fm of the α-like clusters.

Discussion and Conclusions

- In the case of NM potential, the fits are excellent using both unshifted repulsive core with $D_1 = 0$ and shifted repulsive core with $D_1 \neq 0$.

- However, the total χ^2-value $\left(\sum_i \chi_i{}^2 = 3.747\right)$ for potentials with $D_1 = 0$ has been found to be lower than that $\left(\sum_i \chi_i{}^2 = 5.667\right)$ for potentials with $D_1 \neq 0$.

- The potential with $D_1 = 0$ and that with $D_1 \neq 0$ mainly differ in the central region of the target nucleus.

- From the closeness of the fits to the data and the nearly same χ^2-value suggest that the scattering is dominated by potentials at nuclear surface.

- Thus the MSF and NM potentials have been proved to be successful in explaining the α elastic scattering on ^{208}Pb.

THANK YOU FOR YOUR PATIENCE